THE EFFECTS OF SURFACE CORROSION ON THE FATIGUE BEHAVIOUR OF ALUMINIUM ALLOY SPECIMENS CONTAINING COLD EXPANDED HOLES.

N.Glinos, P.G Wagstaff and R.Cook*
Aeronautical Engineering, Kingston University,
DRA Farnborough* U.K.

Abstract

This paper reports on results from an experimental fatigue test programme carried out at Kingston University on specimens of aluminium alloy 7050-T76 which had been affected by pitting corrosion of the surface resulting from normal atmospheric exposure.
Fatigue tests were carried out on specimens containing plain holes and specimens containing holes cold expanded using a commercial split sleeve process. The effect of the surface corrosion on the fatigue endurance has been assessed for plain and cold expanded hole specimens and compared with results obtained for specimens in the uncorroded condition.
The results show that there is a significant reduction in the fatigue endurance of the corroded material for cold expanded holes compared to the fatigue endurance of the uncorroded material. The beneficial effect of cold expansion is still evident in the corroded specimens, but it is less marked than in the uncorroded specimens. These effects were found to be dependent on applied stress levels.
Residual stresses induced by the cold expansion process have been measured at the DRA using an X-ray diffraction technique. Theses stresses have been combined with the applied stresses, derived from a finite element analysis, and used to determine the effective stress range. This has been calculated using Schijve's crack closure corrections. The location of crack initiation and subsequently observed crack growth behaviour are explained qualitatively in terms of the effective stress ranges present.

Introduction

Cold expansion of fastener holes is a well established technique for improving the fatigue endurance of mechanically fastened joints in aircraft structures. The cold expansion process involves pulling a tapered mandrel through a lubricated sleeve inserted in the fastener hole which creates plastic deformation of the material surrounding the hole. This introduces significant compressive residual stresses around the circumference of the fastener hole which leads to an enhancement of the fatigue life of the structure. This compressive residual stress field is balanced by a tensile residual stress zone in an annulus of material surrounding the plastically deformed material. There is concern that fatigue cracks which initiate in this region could propagate rapidly due to the tensile residual stresses present and negate the effectiveness of the cold expansion. The development of cracks in this region could arise, for example, from fretting fatigue between the clamped surfaces in the joint or from defects in the material such as corrosion pits. This is of particular concern in aircraft structures where cold expansion is frequently used as part of repair and modification procedures. In such circumstances, the aircraft will have been subjected to operating environmental conditions and it is possible/probable that the surface of the material may be affected by corrosion damage.

Research work has been undertaken at Kingston University to examine the interaction of residual stresses caused by hole cold expansion and defects caused by corrosion. The research is particularly concerned with the growth of cracks from these defects in cold expanded components subjected to fatigue loading. The initial phase of this work was concerned with establishing whether the effectiveness of hole cold expansion could be compromised by the growth of cracks from corrosion pits in the tensile residual stress region. The results of this initial phase showed that under the conditions chosen, the fatigue endurance of cold expanded corroded specimens was less than 25 % of the endurance of similar non corroded specimens [1]. The work has now been extended to determine the conditions under which these reductions in fatigue life occur, using both experimental and analytical approaches. This report describes the current findings of the work which examines the effectiveness of cold expansion in 7050-T76 aluminium alloy which has been subjected to pitting corrosion arising from normal atmospheric exposure.

Experimental Programme

The initial experimental test programme, described in reference 1, used simple open hole specimens of the type shown in figure 1. Plain holes (designated SR) were drilled and reamed to a diameter of 5.994 mm. Cold expanded holes (designated CX) were initially drilled and reamed to a diameter of 5.994 mm, cold expanded by approximately 4 % using standard FTI tooling and subsequently reamed to 6.312 mm to remove the pip of the material formed in the gap of the split sleeve during cold expansion [2]. The material used was 7050-T76, the chemical and mechanical properties of which are given in Tables 1 and 2 respectively. Specimens were

manufactured from sheets of one batch of material some of which had been stored with protective coatings and some of which had been stored without protective coatings in normal atmospheric conditions for a period of two years. The same material and specimen configuration has been used in the current investigation to establish the conditions under which the effectiveness of cold expansion is reduced due to the growth of cracks from corrosion pits. In the initial programme, fatigue tests were carried out under constant amplitude sinusoidal loading at a stress ratio of R=0.1 and a frequency of 10 Hz. A single value of maximum gross stress, 175 MPa, was used in the initial investigation and the log mean fatigue test endurances are presented in Table 3 for plain and cold expanded holes in plain and corroded material. The reduction in fatigue endurance of cold expanded corroded specimens was caused by failure of the test pieces from cracks originating at corrosion pits. Failure in all of the other tests occurred from cracks originating at the edge of the open hole. It was argued that at lower alternating applied stresses the location of cracks causing failure would also be from corrosion pits, but at higher alternating stresses the location of cracks causing failure would eventually move to the edge of the hole. Additional tests were therefore carried out with maximum gross section stresses of 150 and 200 MPa.

During the fatigue tests crack lengths were monitored on both faces of the specimen by means of a replica technique using cellulose acetate sheet softened with acetone. The replicas were subsequently examined using a "Shadowgraph" projector and the crack lengths measured. This was a very labour intensive method as the possible area in which cracks could initiate and grow was extremely large. However, a large volume of crack growth data was generated as extensive crack initiation at corrosion pits occurred at as many as 100 locations on one specimen.

Specimens manufactured from the non protected sheets of material were examined to determine the extent of the corrosion. These were prepared for examination by etching with a solution containing 2% hydrofluoric acid, 5% nitric acid and 93% distilled water for 60 seconds and then examined using an optical microscopic. Measurements were made of the surface pit size, shape and depth and the typical pit density. Examinations were also made of the surfaces of cold expanded corroded specimens to establish whether the cold expansion process caused cracking of the pits. This was achieved by examining pits at various locations on the specimen surfaces close to and remote from the hole.

Analytical programme

The aims of the analytical programme were to establish why fatigue cracks initiated and grew at the experimentally determined locations, and to predict the effect of applied load on the location of the cracks causing failure. A fracture mechanics approach was used to establish the crack driving forces at the locations of interest. This required evaluation of the stress distributions associated with the central hole and corrosion pits, under externally applied loading. The residual stresses associated with the cold expansion process also had to be considered in the fracture mechanics approach. It is anticipated that this approach will be developed further to predict crack growth rates from the critical locations and compare them with the experimental measurements described earlier.

The stress distribution due to the externally applied loading was determined using a Nisa III Finite Element Model (FEM). Detailed stress analyses were performed over a large area of the specimen as stress distributions were required in all of the potential crack initiation sites. One quarter of the specimen only was modelled assuming symmetry on both X and Y planes.

The total stress at any location in the specimen is the sum of the applied and the residual stress due to cold expansion. A number of investigators have determined the residual stresses surrounding cold expanded holes using a variety of experimental and analytical techniques [3,4,5,6,7]. Most analytical approaches have used elasto-plastic Finite or Boundary Element methods, and have generally been two dimensional models which assume uniform radial expansion of the hole. The residual stresses obtained from these models are not representative of the true stresses present. These have been shown in previous investigations to vary through the specimen thickness and with angular location around the hole in addition to varying with distance away from the hole. The 2D analyses with uniform radial expansion can clearly only give stress variations with distance away from the hole. A full 3D calculation, with modelling of the split sleeve and the mandrel would be required to provide an accurate evaluation of the stresses around a cold expanded hole. This would be extremely expensive and would require considerable computational effort. The experimental determinations of residual stresses have generally used X-ray diffraction, Neutron diffraction and more recently Sachs boring methods. Each process has its limitations in terms of resolution and measurement location. The locations of interest in this investigation are the surfaces of the specimens where X-ray methods are most appropriate. Consequently measurements of residual stresses using X-ray diffraction have been used in the analytical programme. The limitations of the technique relate to the dimensions of the X-ray beam. The stress measurement at any location represents some average of the stresses present in the area irradiated by the beam, which becomes important in areas of high stress gradient. It is also difficult to measure stresses close to the hole as the volume of material irradiated by the beam will include part of the hole as hole is approached. In this investigation, results of X-ray diffraction measurements

have been modified to more accurately represent the stress distribution close to the hole including the compressive yielding which occurs during mandrel removal. The true residual stress distribution was then estimated by compensating for the averaging effect of the X-ray method. The modified hoop stress distributions on the two faces of the specimen are presented in figure 2. Successive averaging of the distribution shown in figure 2 over the beam length are in good agreement with the original raw X-ray measurements. The face on which the cold expansion mandrel enters the specimens is designated the mandrel inlet face and the face on which the mandrel exits the specimen is designated the mandrel outlet face. These distributions were measured along the minimum section of the specimen where cracks would be expected to grow. A more accurate method would include the variation of residual stresses with angular location around the hole, but insufficient data was available.

The residual and applied stress fields were combined by simple addition. This required some further simple calculations as the applied stresses from the Finite Element Model were given in Cartesian co-ordinates and the hoop and radial residual stresses were given in polar co-ordinates. The resultant stresses were calculated in Cartesian co-ordinates for any applied loading range.

In order to compare the effect of these stress fields on the growth of cracks, it was necessary to determine the effective crack driving forces at locations of interest. The driving force is a function of the effective stress range, the crack length and the geometry of the specimen. For simplicity, a common pit shape and initial crack length was assumed in all areas of the specimen, such that the driving force was only dependent on the effective stress range. The assumption of common pit shape and size was investigated by optical microscopy, described earlier, and the probability of pits being present at all of the locations of interest was examined by measurements of pit density, also described earlier. The assumption that small cracks would be present at the pits was examined by optical microscopy of specimens subjected to alternating loading and the size of cracks present was also measured as described later in the results. The driving forces were thus assumed only to be dependent on the effective stress range which was calculated using the total stress distributions described above (sum of the applied and residual stress distributions). The effective stress range ($\Delta\sigma$eff) was calculated using the crack opening stress correction proposed by Schijve[8] and assuming that cracks would only be affected by the stress in the loading direction (σyy), i.e. assuming that Mode I cracks only would grow.

$\Delta\sigma eff = [\sigma yy(app)(max) + \sigma yy(res)](1-\sigma(op)/\sigma(max))$
where $= \sigma(op)/\sigma(max) = 0.1R^3 + 0.25R^2 + 0.2R + 0.45$
and R = Stress ratio, $\sigma(op)$ = opening stress,
$\sigma yy(app)$ = applied stress, $\sigma yy(res)$ = residual stress

Results

a. Experimental programme

The fatigue test endurances measured during the current and previous investigations for plain and cold expanded hole specimens manufactured from corroded and uncorroded materials are presented in Table 3. It can be seen that at a stress level of 175 MPa, cold expansion of uncorroded material extends the fatigue life endurance by a factor of about 20 but for corroded materials the improvement is only by a factor of 3; this is shown schematically in Table 4. This is accounted for by the failures of cold expanded corroded materials originating at corrosion pits remote from the holes causing premature failure. It is also worthy of note that the failure originated at the mandrel inlet face for cold expanded non-corroded specimens but that the majority of failures in cold expanded corroded specimens originated on the mandrel outlet face. This is to be expected as the residual stresses adjacent to the hole (see figure 2) are less compressive on the mandrel inlet face compared with the outlet face and therefore failures from the hole are expected to initiate from the mandrel inlet face. Remote from the hole, however, the tensile residual stresses are greater on the mandrel outlet face than on the mandrel inlet face, so failures are expected from the mandrel outlet face.
At the higher applied stress of 200 MPa, the failure location in corroded specimens was from the central hole and therefore the effect of the corrosion is likely to be less marked. At the lower stress level of 150 MPa the failure was from corrosion pits remote from the hole, as expected, and the influence of corrosion is expected to be more marked than at the higher stress levels.

b. Analytical programme

The effective stress ranges calculated using the analyses described above are presented in Tables 5 and 6 for the mandrel outlet and inlet faces respectively. Also presented in these tables are the effective stress ranges normalised by the applied stress range which are shown as the ratio A. This ratio has been calculated to make comparisons between the various applied stress levels more straightforward in that the applied stresses can be ignored and the relative stress severity compared at various locations. The values of zero in the table indicate that the entire stress range is compressive. The highest values in the table represent the highest effective stress regions where cracks would be expected to propagate. The highlighted areas in the tables are where effective stress ratios exceed 0.68 and can be considered as the 'hot-spots' for crack initiation and growth. Thus at 150 MPa, it can be seen that the highest effective stress occurs at the hole edge on the inlet face but that this decreases rapidly away from the hole. Significant effective stresses are also found at regions remote from the hole (3.5 to 7 mm from

the hole) and that these are higher on the mandrel outlet face than on the mandrel inlet face. Similar results are found at the other two stress levels except that significant effective stresses are also found close to the hole on the mandrel outlet face.

c. Examination of specimen surfaces

Corrosion pits were examined to determine their size, shape and density. The pits examined had a wide range of shapes, the surface areas varying from 1.021×10^{-4} mm^2 to 5.08×10^{-2} mm^2 and depths varying from 13 μm to 110 μm. The majority of pits examined had a surface area of about 5×10^{-4} mm^2 and a depth of about 25 μm. The average density of pits was found to be about 10^6 per m^2. Some typical examples of corrosion pits of different sizes on the specimen surfaces are shown in figures 3, 4 and 5. After cold expansion, little difference was found to the pits and no evidence of cracking was found. Examination of the specimen surfaces during tests enabled determination of the location and size of fatigue cracks present. Some examples of fatigue cracks emanating from corrosion pits are shown in figure 6. The location of cracks which started from corrosion pits and caused fatigue failure are summarised for all tests on cold expanded specimens in figures 7 and 8 for the mandrel inlet and outlet faces respectively.

The location of additional cracks from pits which did not cause failure are presented in figures 9 and 10 for the mandrel inlet and outlet faces respectively. Also shown on these figures are the effective stress ranges described earlier. It can be seen that the majority of cracks which caused failure (see figs 7 and 8) initiated in regions where the effective stress range was greater than 105 MPa and that the majority of cracks which did not cause failure (see figs 9 and 10) initiated where the range was greater than 85 MPa. Cracks were generally found in the sector between +/- 45 degrees from the specimens transverse axis. The size distribution and location of cracks which did not cause failure are summarised in Table 7. It can be seen that the majority of the cracks remote from the hole seldom grew to a length of greater than 1 mm, as did cracks from the hole on the mandrel outlet size. In contrast, more than half of the cracks growing from the hole on the mandrel inlet face grew to a length greater than 1 mm but none were greater than 2 mm.

Discussion

The initial growth of cracks from corrosion pits is controlled by the effective stress range present. The calculation of effective stress range over the surfaces of cold expanded test specimens highlighted areas, other than the edge of the central hole, where the effective stress range was large. These areas corresponded well with the locations of the fatigue cracks found in the experimental phase of the work (see figs 7 and 8). The location of cracks which cause specimen failure are controlled by the effective stress range being consistently high in the region of crack propagation. Thus although the effective stress range is always highest at the edge of the hole on the specimen inlet side (see Table 6), because the stress range decays rapidly, failure does not always occur from cracks at this location. It can be seen that although the stress range is somewhat lower at locations remote from the hole (indicated by bold print in Tables 5 and 6), the range remains consistently high in this region and cracks which cause failure frequently initiate in this area. This area is referred to as 'Region 1'. A comparison of the stress severity at different applied stresses (see Tables 5 and 6) shows that the severity of the stresses remote from the hole in the region 1 are relatively unaffected by applied stress level, for example on the mandrel inlet face the values range from 0.68 to 0.76 at all three stress levels. In contrast with increasing applied loads the stress severity increases near the edge of the hole and consequently at higher applied loads the location of cracks which cause failure changes from a remote failure to a hole failure.

The propagation of fatigue cracks was monitored throughout the fatigue tests. Multiple cracks were observed in all tests, particularly in region 1. The growth of cracks from corrosion pits in this region was complex. Due to the density of pits many cracks formed in this region though the majority (84%) failed to propagate to lengths greater than 1 mm. This is due to the local stress concentration of the pit which raises the local stresses sufficiently to cause initial crack growth but the stress intensification decays rapidly away from the pit, which combined with a general decrease in the effective stress range, causes the cracks to slow and arrest. Cracks causing failure, which initiated in this region, were generally located on the mandrel outlet face where the effective stress range was higher than on the mandrel inlet face. Fatigue crack growth in the early stages consisted of linking of cracks at corrosion pits. Merging generally occurred with cracks of less than 1 mm in length, resulting in irregular crack growth rate as cracks accelerated towards each other then decelerated after merging. Growth through the thickness could not be monitored, but surface breaking cracks could be monitored when the main crack broke through to the opposite face. Frequently the main crack also eventually merged with the main crack growing from the central hole. This growth pattern would make prediction of fatigue crack growth rates extremely complicated but work towards a general model will be pursued. This will be targeted initially at prediction of the location of the crack which causes failure.

The fatigue endurances of specimens tested in this programme are presented in Table 3. The effectiveness of hole cold expansion is clear from the tests conducted at 175 MPa where a life improvement factor of about 20 was

achieved for non corroded material. The life improvement is dependent on a number of factors but is particularly sensitive to the externally applied loading. Previous work on a similar specimens and material using the same stress ratio showed that cold expansion improved the fatigue endurance by a factor of 2 at high stress levels, increasing to a factor of 70 close to the endurance limit of the cold expanded specimens [4]. It also showed that the endurance limit for cold expanded holes was greater than for plain holes, though arrested fatigue cracks were present in cold expanded specimens tested at stresses below the endurance limit. This is in good agreement with the results from this investigation where at 175 MPa (close to the fatigue limit), a life improvement factor of 20 was achieved. The importance of corrosion can be seen from Table 4 where this life improvement factor was reduced to 3 by the presence of corrosion. At higher stress levels, however, the benefits of cold expansion are less marked, and since the corrosion does not cause premature failure of the specimen from corrosion pits, the importance of corrosion in reducing the effectiveness of cold expansion will become less important. In contrast, at lower stress levels, the effectiveness of cold expansion is greater and premature failures occur due to cracks initiating at corrosion pits, so the importance of corrosion in reducing the effectiveness of cold expansion becomes more important.

This is the area of most significance to the aircraft industry where, for safety and durability reasons, the stresses are generally low. It can be expected, therefore, that if corrosion is present in aircraft structures which are cold expanded as part of a repair or modification process, the effectiveness of the cold expansion could be considerably less than expected. Furthermore, conventional examination of the structure for cracks emanating from fastener holes will not detect the important cracks present, which cause failure, as they initiate remote from the hole. Cracks which cause failure in cold expanded corroded material also generally will be on the opposite side of the structure from the cracks which cause failure in cold expanded non corroded material, where inspections will be focused.

Conclusions

1. The effectiveness of cold expansion as a life enhancement technique is seriously affected by the presence of surface corrosion in 7050-T76 material.
2. Cracks growing from corrosion pits remote from cold expanded holes can cause premature specimen failure at low applied alternating stresses.
3. Such crack initiation sites correlate well with regions of high effective stress range calculated from a summation of applied and residual stresses accounting for crack closure.
4. There are important implications for the inspection of cold expanded fastener holes since the cracks which cause eventual failure in corroded material initiate in regions remote from the edge of the hole, and on the opposite face to that in non-corroded material.
5. There is no evidence that cracks are formed at corrosion pits during the cold expansion process.

References

1. N.Glinos, P.G.Wagstaff and R.Cook, *The effects of surface corrosion on the fatigue behaviour of aluminium alloy specimens containing cold expanded holes.* C M T 96. Pub C M P, Southampton, UK, 1996.

2. M.A Landy and R.L Champoux *FTI Engineering process specification FTI 8108B*, 1984, Seattle, USA, Fatigue Technology, Inc.

3. D.L.Rich and L.F.Impellizzeri, *Fatigue analysis of cold-worked and interference fit fastener holes.* McDonnell Aircraft Company Report MCAIR 76-007, 1976.

4. A.T.Ozdemir, R.Cook and L.Edwards *Residual stress distributions around cold expanded holes.* Durability and Structural Integrity of Airframes. Vol. I, Pub EMAS, Wharley, UK, 1993.

5. V.Leitao. M.H.Aliabadi, D.P.Rooke and R.Cook, *Residual stress fields effect on fatigue crack growth.* Boundary Element XIV Vol.2, Pub C M P, Southampton, UK, 1992.

6. R.Cook, P.Holdway, *Residual stresses induced by hole cold expansion.* Computer methods and Experimental Measurements for Surface Treatment Effects. Pub C M P, Southampton, UK 1993.

7. L.Edwards and A.T.Ozdemir, *Residual stresses at cold expanded fastener holes.* Measurement of residual and applied stress using Neutron diffraction. Pub. Kluwer Academic Publishers,1992.

8. J.Schijve, *The stress ratio effect on fatigue crack growth in 2024-T3 aclad and the relation to crack closure.* Delft University of Technology, Memorandum M-336, 1979.

Acknowledgements

The authors would like to thank the Structural Materials Centre, DRA and Kingston University for their support for this work.

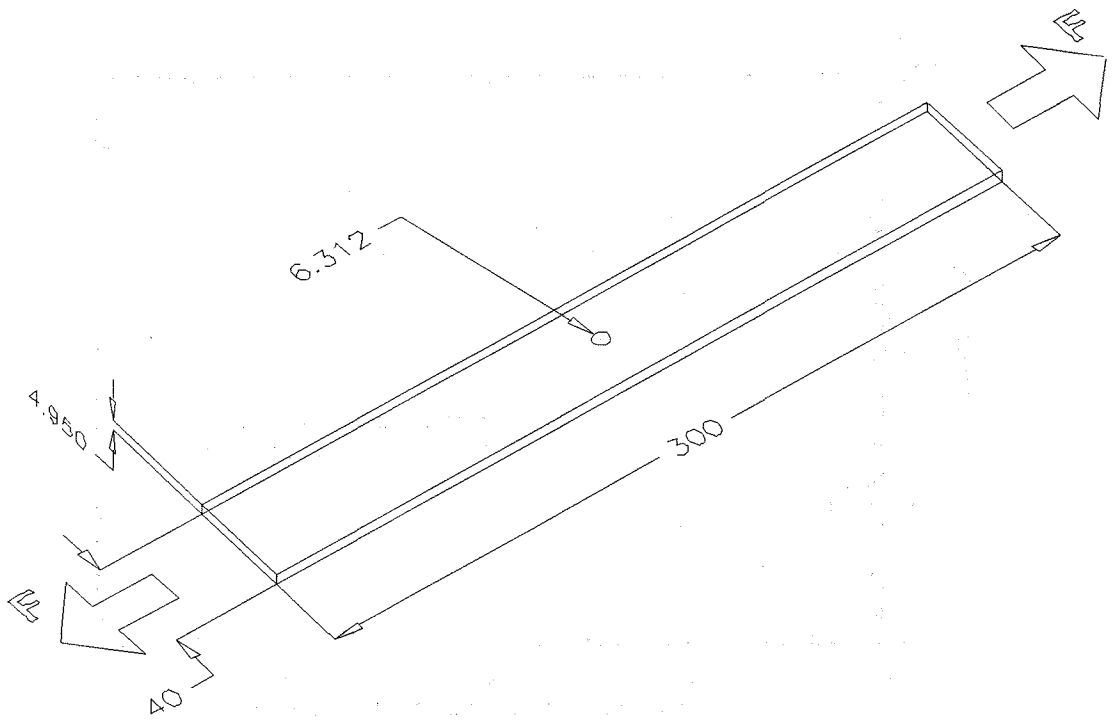

Fig. 1 Fatigue test specimen (in mm)

	Al	Cr	Cu	Fe	Mg	Mn	Si	Ti	Zn	Zr
Min	90.4	-	1.9	-	1.9	-	-	-	5.7	0.08
Max	87.4	0.04	2.6	0.15	2.6	0.1	0.12	0.06	6.7	0.15

Table 1. Chemical composition of 7050-T76

0.2% yield stress	UTS	Elongation	Modulus of Elasticity
555 MPa	582 MPa	11%	69.5 GPa

Table 2. Mechanical properties of 7050-T76

Stress levels (MPa)	Cold expanded uncorroded specimen	Cold expanded corroded specimen	Plain uncorroded specimen	Plain corroded specimen
150	-	159850	-	-
175	507818	119874	22420	28418
200	-	84130	-	-

Table 3. Log mean fatigue test endurances

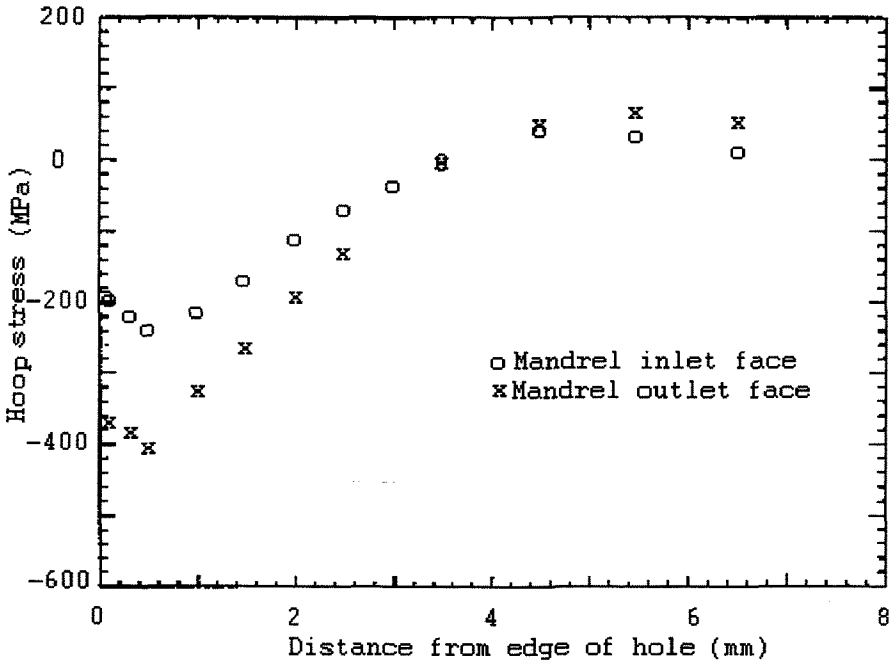

Fig. 2 Residual hoop stresses induced by the cold expansion process.

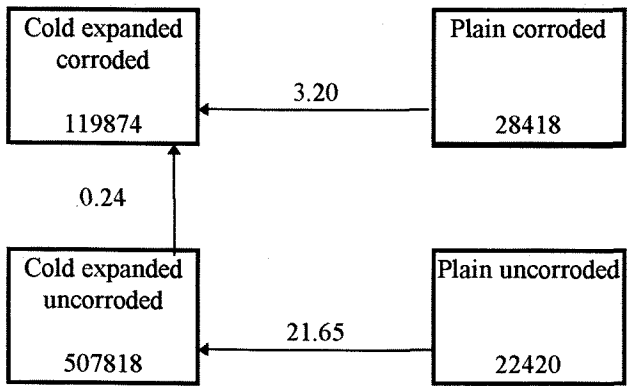

Table 4. Life improvement ratio of Log mean endurances (cycles)

Distance from edge of the hole (mm)	150 MPa		175 MPa		200 MPa	
	Δσeff	A	Δσeff	A	Δσeff	A
0.000	0.000	0.000	119.315	0.758	155.996	0.867
0.500	0.000	0.000	0.000	0.000	0.000	0.000
1.000	0.000	0.000	0.000	0.000	0.000	0.000
2.000	0.000	0.000	0.000	0.000	61.439	0.341
3.000	72.521	0.537	90.319	0.573	107.783	0.599
3.500	92.385	**0.684**	108.503	**0.689**	124.614	**0.692**
4.000	100.375	**0.744**	116.037	**0.737**	131.665	**0.731**
4.500	102.698	**0.761**	118.253	**0.751**	133.750	**0.743**
5.000	103.678	**0.768**	119.039	**0.756**	134.304	**0.746**
5.500	103.639	**0.768**	118.925	**0.755**	134.105	**0.745**
6.000	101.610	**0.753**	116.611	**0.740**	131.509	**0.731**
7.000	97.547	**0.723**	112.132	**0.712**	126.643	**0.704**
8.000	90.552	0.671	104.741	0.665	118.911	0.661
9.000	89.808	0.665	103.866	0.659	117.906	0.655
10.000	83.065	0.615	96.910	0.615	110.754	0.615
11.000	82.274	0.609	95.987	0.609	109.699	0.609
12.000	81.483	0.604	95.064	0.604	108.644	0.604
13.000	80.692	0.598	94.141	0.598	107.590	0.598
14.000	79.901	0.592	93.218	0.592	106.535	0.592
15.000	79.110	0.586	92.295	0.586	105.480	0.586
16.844	76.737	0.568	89.526	0.568	102.316	0.568

Table 5. Δσeff and A values / Mandrel outlet face

Distance from edge of the hole (mm)	150 MPa		175 MPa		200 MPa	
	Δσeff	A	Δσeff	A	Δσeff	A
0.000	162.160	1.201	206.854	1.313	250.428	1.391
0.500	76.087	0.564	99.933	0.634	134.220	0.746
1.000	0.000	0.000	0	0.000	0.000	0.000
2.000	59.615	0.442	80.983	0.514	101.863	0.566
3.000	86.878	0.644	103.784	0.659	120.610	0.670
3.500	94.648	**0.701**	110.741	**0.703**	126.832	**0.705**
4.000	99.963	**0.740**	115.614	**0.734**	131.242	**0.729**
4.500	101.745	**0.754**	117.256	**0.744**	132.718	**0.737**
5.000	99.068	**0.734**	114.175	**0.725**	129.236	**0.718**
5.500	97.993	**0.726**	112.958	**0.717**	127.879	**0.710**
6.000	92.993	**0.689**	107.577	**0.683**	122.142	**0.679**
7.000	88.894	0.658	103.161	0.655	117.422	0.652
8.000	90.902	0.673	105.101	0.667	119.278	0.663
9.000	89.808	0.665	103.866	0.659	117.906	0.655
10.000	83.065	0.615	96.91	0.615	110.754	0.615
11.000	82.274	0.609	95.987	0.609	109.699	0.609
12.000	81.483	0.604	95.064	0.604	108.644	0.604
13.000	80.692	0.598	94.141	0.598	107.590	0.598
14.000	79.901	0.592	93.218	0.592	106.535	0.592
15.000	79.110	0.586	92.295	0.586	105.480	0.586
16.844	76.737	0.568	89.526	0.568	102.316	0.568

Table 6. Δσeff and A values / Mandrel inlet side

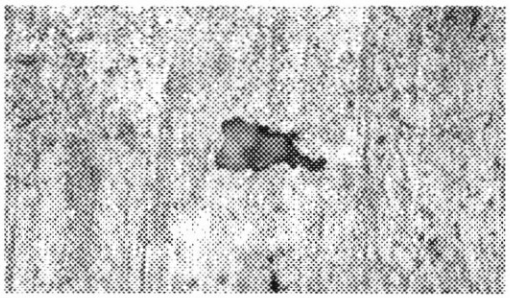

Fig.3. Typical corrosion pit (a)

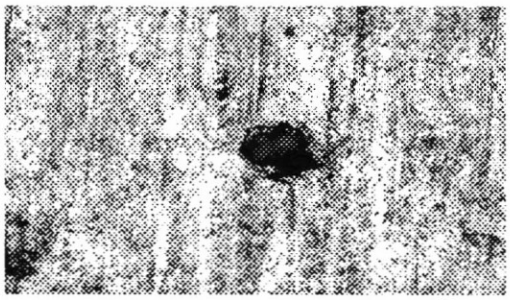

Fig.4. Typical corrosion pit (b)

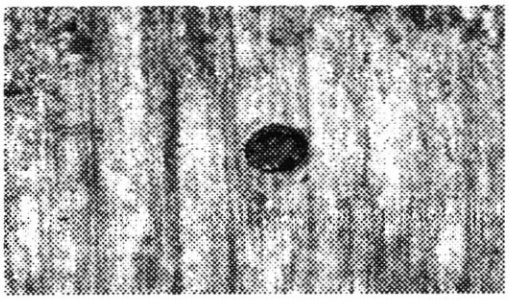

Fig.5. Typical corrosion pit (c)

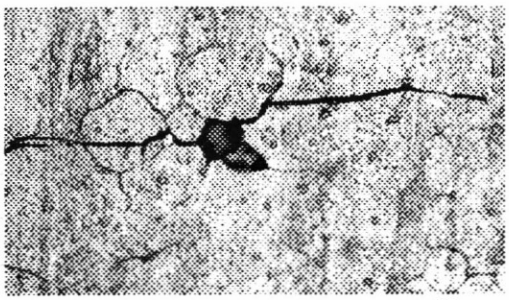

Fig.6. Crack emanating from a corrosion pit

	a < 1mm	1 £ a < 2 mm	2 mm £ a
Additional cracks (inlet and outlet side)	83.91 %	12.61 %	3.48 %
Hole (inlet side)	42.43 %	57.57 %	0
Hole (outlet side)	97.30 %	2.70 %	0

Table 7. Size distribution and location of cracks.

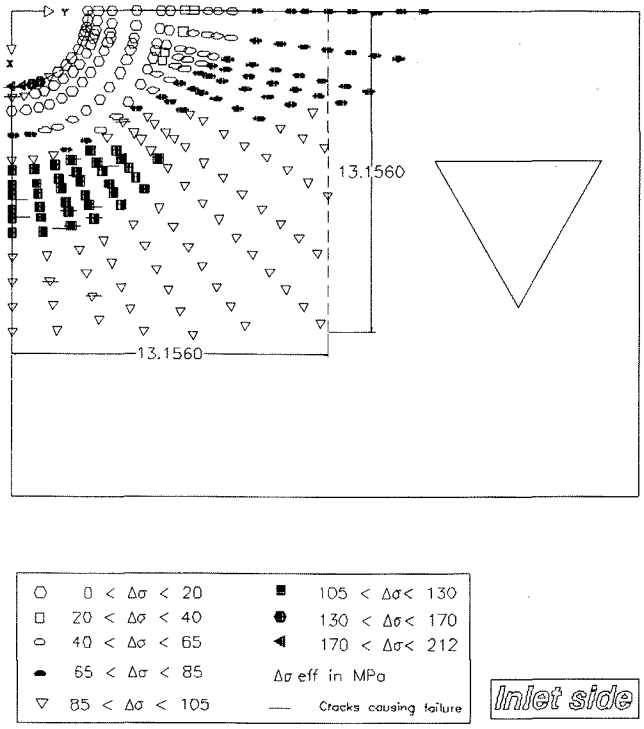

Fig 7. The distribution of $\Delta\sigma_{eff}$ and the cracks causing failure (Mandrel inlet face).

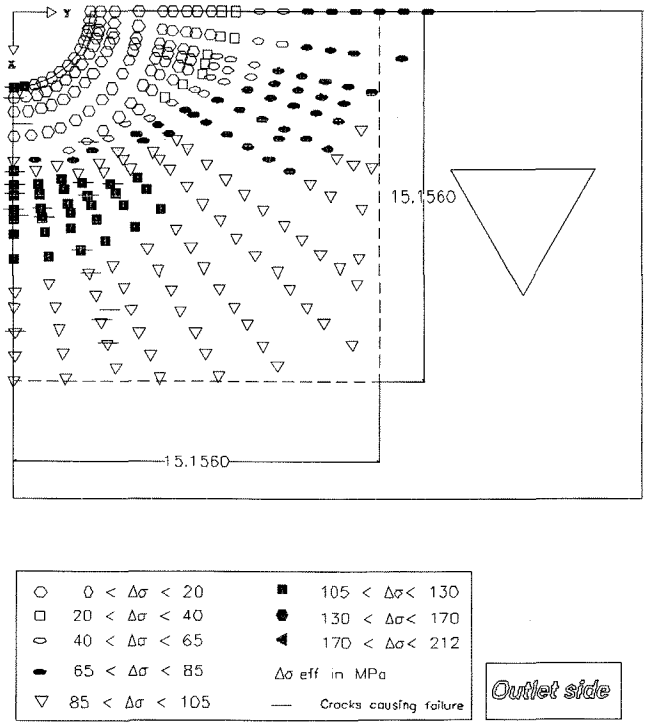

Fig. 8 The distribution of $\Delta\sigma_{eff}$ and the cracks causing failure (Mandrel outlet face).

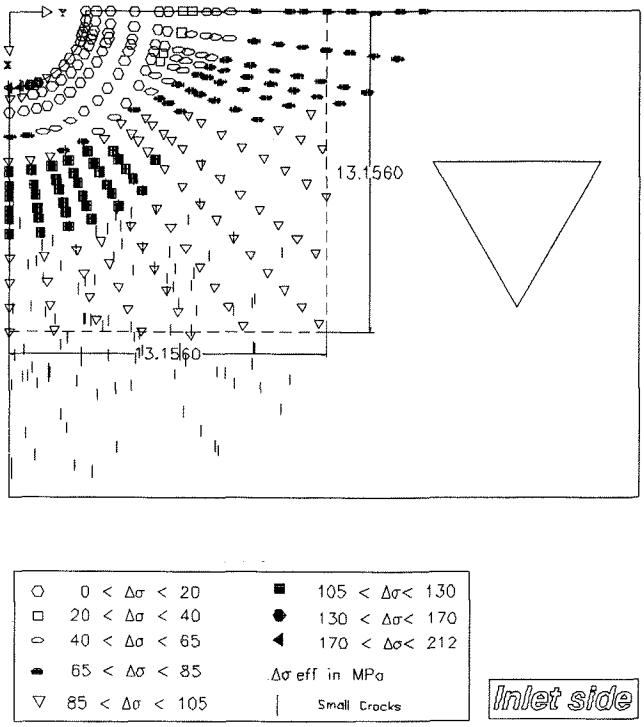

Fig. 9 The distribution of $\Delta\sigma_{eff}$ and the additional cracks (Mandrel inlet face).

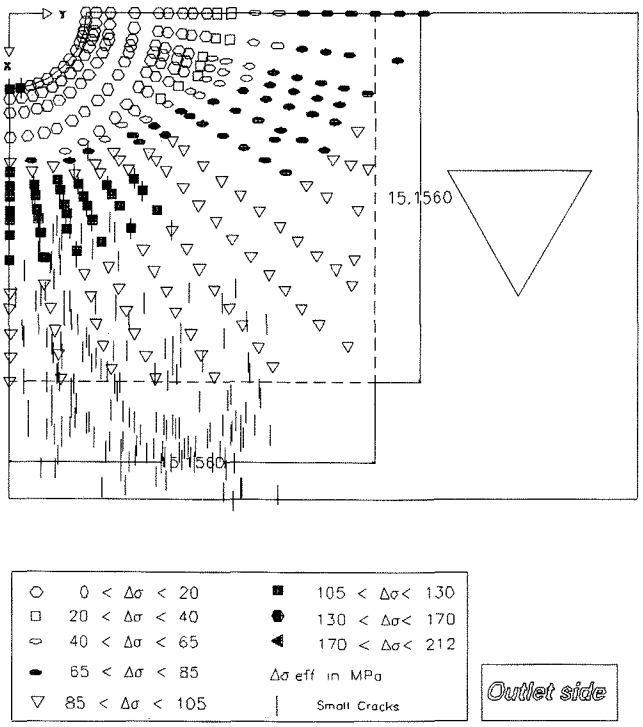

Fig. 10 The distribution of $\Delta\sigma_{eff}$ and the additional cracks (Mandrel outlet face).